Supplement: Ab Initio Finite Temperature Auxiliary Field Quantum Monte Carlo

Yuan Liu, Minsik Cho, and Brenda Rubenstein*
Department of Chemistry, Brown University, Providence Rhode Island 02912, USA

A. The Continuous Hubbard-Stratonovich Transformation of an *Ab Initio* Hamiltonian

In this section, we provide more details regarding the manipulation of the *ab initio* Hamiltonian that makes it amenable to a continuous Hubbard-Stratonovich Transformation. As described in the main text, after recasting the two body interaction term into a density-density form, a supermatrix, $V_{(i\alpha,k\alpha),(l\beta,j\beta)}$ may be formed and diagonalized (or decomposed) into

$$V_{(i\alpha,k\alpha),(l\beta,j\beta)} = \sum_{\gamma}^{(2N)^2} R_{(i\alpha,k\alpha)\gamma}\lambda_\gamma R^*_{(l\beta,j\beta)\gamma}, \tag{1}$$

where λ_γ is the γ-th eigenvalue, and $R_{(i\alpha,k\alpha)\gamma}$ is the $(i\alpha,k\alpha)$-th element of the γ-th eigenvector. The two body term then becomes

$$\begin{aligned}\frac{1}{2}\sum_{i\alpha,j\beta,k\alpha,l\beta}^{2N} V_{(i\alpha,k\alpha),(j\beta,l\beta)}c^\dagger_{i\alpha}c_{k\alpha}c^\dagger_{j\beta}c_{l\beta} &= \frac{1}{2}\sum_{i\alpha,j\beta,k\alpha,l\beta}^{2N}\sum_{\gamma}^{(2N)^2} R_{(i\alpha,k\alpha)\gamma}\lambda_\gamma R^*_{(l\beta,j\beta)\gamma}\big(c^\dagger_{i\alpha}c_{k\alpha}\big)\big(c^\dagger_{j\beta}c_{l\beta}\big)\\ &= \frac{1}{2}\sum_{\gamma}^{(2N)^2}\lambda_\gamma\Big(\sum_{i\alpha,k\alpha}^{2N} R_{(i\alpha,k\alpha)\gamma}(c^\dagger_{i\alpha}c_{k\alpha})\Big)\Big(\sum_{j\beta,l\beta}^{2N} R^*_{(l\beta,j\beta)\gamma}(c^\dagger_{j\beta}c_{l\beta})\Big),\end{aligned} \tag{2}$$

where the creation and annihilation operators follow the definition in the main text.

Following Zhang, it may be recognized that $\sum_{j\beta,l\beta}^{2N} R^*_{(l\beta,j\beta)\gamma}(c^\dagger_{j\beta}c_{l\beta})$ and $\sum_{i\alpha,k\alpha}^{2N} R_{(i\alpha,k\alpha)\gamma}(c^\dagger_{i\alpha}c_{k\alpha})$ are simply Hermitian conjugates of each other. We can therefore write the two body potential operator, $\hat{V}$, as

$$\hat{V} = \frac{1}{2}\sum_{\gamma}^{(2N)^2}\lambda_\gamma\hat{\rho}_\gamma\hat{\rho}^\dagger_\gamma - \frac{1}{2}\sum_{\alpha}\hat{\rho}^\alpha_0, \tag{3}$$

where

$$\hat{\rho}_\gamma = \sum_{i\alpha,k\alpha}^{2N} R_{(i\alpha,k\alpha)\gamma}(c^\dagger_{i\alpha}c_{k\alpha}), \tag{4}$$

and

$$\hat{\rho}^\alpha_0 = \sum_{ij}^{N}\Big(\sum_{k}^{N} V^{\alpha\alpha\alpha\alpha}_{ikkj}\Big)c^\dagger_{i\alpha}c_{j\alpha}. \tag{5}$$

It is straightforward to see that Hermiticity guarantees that

$$\hat{\rho}_\gamma\hat{\rho}^\dagger_\gamma = \hat{\rho}^\dagger_\gamma\hat{\rho}_\gamma. \tag{6}$$

It follows that Equation (3) may be re-expressed as

* brenda_rubenstein@brown.edu

$$\hat{V} = \frac{1}{4}\sum_{\gamma}^{(2N)^2} \lambda_\gamma \{\hat{\rho}_\gamma, \hat{\rho}_\gamma^\dagger\} - \frac{1}{2}\sum_{\alpha}\hat{\rho}_0^\alpha \tag{7}$$

$$= \frac{1}{8}\sum_{\gamma}^{(2N)^2} \lambda_\gamma [(\hat{\rho}_\gamma + \hat{\rho}_\gamma^\dagger)^2 - (\hat{\rho}_\gamma - \hat{\rho}_\gamma^\dagger)^2] - \frac{1}{2}\sum_{\sigma}\hat{\rho}_0^\alpha. \tag{8}$$

$\hat{\rho}_0^\alpha$ is a one body term and can be readily combined with the original one body term $\hat{K}$. The total Hamiltonian may now be expressed as

$$\hat{H} = \sum_{\alpha}\hat{H}_{1\alpha} + \hat{H}_2, \tag{9}$$

in which

$$\hat{H}_{1\alpha} = \sum_{ij}^{N} T_{i\alpha,j\alpha}\hat{c}_{i\alpha}^\dagger \hat{c}_{j\alpha} - \mu\sum_{i}^{N}\hat{c}_{i\alpha}^\dagger\hat{c}_{j\alpha} - \frac{1}{2}\hat{\rho}_0^\alpha, \tag{10}$$

$$\hat{H}_2 = \frac{1}{8}\sum_{\gamma}^{(2N)^2}\lambda_\gamma[(\hat{\rho}_\gamma + \hat{\rho}_\gamma^\dagger)^2 - (\hat{\rho}_\gamma - \hat{\rho}_\gamma^\dagger)^2]. \tag{11}$$

Observe that $\hat{H}_2$ is now a summation of squares of one body terms, and can be decoupled using the continuous Hubbard-Stratonovich Transformation in the following way

$$\begin{aligned} e^{-\triangle\tau\hat{H}_2} &= e^{-\frac{\triangle\tau}{8}\sum_\gamma^{(2N)^2}\lambda_\gamma(\hat{\rho}_\gamma+\hat{\rho}_\gamma^\dagger)^2} e^{\frac{\triangle\tau}{8}\sum_\gamma^{(2N)^2}\lambda_\gamma(\hat{\rho}_\gamma-\hat{\rho}_\gamma^\dagger)^2} \\ &= \prod_{\gamma}^{(2N)^2}\left(\frac{1}{\sqrt{2\pi}}\right)^2\int_{-\infty}^{\infty}\int_{-\infty}^{\infty} d\phi_{\gamma-}d\phi_{\gamma+} e^{-\frac{\phi_{\gamma+}^2+\phi_{\gamma-}^2}{2}} e^{i\frac{\sqrt{\triangle\tau\lambda_\gamma}}{2}\phi_{\gamma+}(\hat{\rho}_\gamma+\hat{\rho}_\gamma^\dagger)} e^{\frac{\sqrt{\triangle\tau\lambda_\gamma}}{2}\phi_{\gamma-}(\hat{\rho}_\gamma-\hat{\rho}_\gamma^\dagger)}. \end{aligned} \tag{12}$$

The propagator can be further split into the spin up and down contributions,

$$\hat{B}_\uparrow(\phi_{\gamma+},\phi_{\gamma-})\hat{B}_\downarrow(\phi_{\gamma+},\phi_{\gamma-}) = e^{i\frac{\sqrt{\triangle\tau\lambda_\gamma}}{2}\phi_{\gamma+}(\hat{\rho}_\gamma+\hat{\rho}_\gamma^\dagger)} e^{\frac{\sqrt{\triangle\tau\lambda_\gamma}}{2}\phi_{\gamma-}(\hat{\rho}_\gamma-\hat{\rho}_\gamma^\dagger)}, \tag{13}$$

where

$$\hat{B}_\uparrow(\phi_{\gamma+},\phi_{\gamma-}) = e^{i\frac{\sqrt{\triangle\tau\lambda_\gamma}}{2}\phi_{\gamma+}\left(\sum_{i\uparrow,k\uparrow}^{N} R_{(i\uparrow,k\uparrow)\gamma}c_{i\uparrow}^\dagger c_{k\uparrow} + \sum_{i\uparrow,k\uparrow}^{N} R_{(i\uparrow,k\uparrow)\gamma}^* c_{k\uparrow}^\dagger c_{i\uparrow}\right)} e^{\frac{\sqrt{\triangle\tau\lambda_\gamma}}{2}\phi_{\gamma-}\left(\sum_{i\uparrow,k\uparrow}^{N} R_{(i\uparrow,k\uparrow)\gamma}c_{i\uparrow}^\dagger c_{k\uparrow} - \sum_{i\uparrow,k\uparrow}^{N} R_{(i\uparrow,k\uparrow)\gamma}^* c_{k\uparrow}^\dagger c_{i\uparrow}\right)} \tag{14}$$

$$\hat{B}_\downarrow(\phi_{\gamma+},\phi_{\gamma-}) = e^{i\frac{\sqrt{\triangle\tau\lambda_\gamma}}{2}\phi_{\gamma+}\left(\sum_{i\downarrow,k\downarrow}^{N} R_{(i\downarrow,k\downarrow)\gamma}c_{i\downarrow}^\dagger c_{k\downarrow} + \sum_{i\downarrow,k\downarrow}^{N} R_{(i\downarrow,k\downarrow)\gamma}^* c_{k\downarrow}^\dagger c_{i\downarrow}\right)} e^{\frac{\sqrt{\triangle\tau\lambda_\gamma}}{2}\phi_{\gamma-}\left(\sum_{i\downarrow,k\downarrow}^{N} R_{(i\downarrow,k\downarrow)\gamma}c_{i\downarrow}^\dagger c_{k\downarrow} - \sum_{i\downarrow,k\downarrow}^{N} R_{(i\downarrow,k\downarrow)\gamma}^* c_{k\downarrow}^\dagger c_{i\downarrow}\right)} \tag{15}$$

are the up and down propagators for one site within one imaginary time step, respectively. Putting this altogether, the total propagator for one imaginary time step for the spin sector α is

$$\hat{B}_\alpha(\vec{\phi}) = e^{-\frac{\triangle\tau\hat{H}_{1\alpha}}{2}}\left[\prod_{\gamma=1}^{(2N)^2}\hat{B}_\alpha(\phi_{\gamma+},\phi_{\gamma-})\right]e^{-\frac{\triangle\tau\hat{H}_{1\alpha}}{2}}, \alpha = \{\uparrow,\downarrow\}. \tag{16}$$

B. Details of the Background Subtraction

To reduce the phase problem, we can further subtract $\langle\hat{\rho}_\gamma + \hat{\rho}_\gamma^\dagger\rangle$ and $\langle\hat{\rho}_\gamma - \hat{\rho}_\gamma^\dagger\rangle$ from (11). In this case, the two body term becomes

$$\frac{1}{8}\sum_{\gamma}^{(2N)^2}\lambda_\gamma\left[(\hat{\rho}_\gamma + \hat{\rho}_\gamma^\dagger)^2 - (\hat{\rho}_\gamma - \hat{\rho}_\gamma^\dagger)^2\right] = \hat{H}_2 + \frac{1}{4}\hat{\eta}_+ - \frac{1}{4}\hat{\eta}_- - \frac{1}{8}\hat{\eta}_0, \tag{17}$$

where

$$\hat{H}_2 = \frac{1}{8}\sum_{\gamma}^{(2N)^2} \lambda_\gamma \Big\{ \big[(\hat{\rho}_\gamma + \hat{\rho}_\gamma^\dagger) - \langle \hat{\rho}_\gamma + \hat{\rho}_\gamma^\dagger \rangle\big]^2 - \big[(\hat{\rho}_\gamma - \hat{\rho}_\gamma^\dagger) - \langle \hat{\rho}_\gamma - \hat{\rho}_\gamma^\dagger \rangle\big]^2 \Big\} \tag{18}$$

$$\hat{\eta}_+ = \sum_{\gamma}^{(2N)^2} \lambda_\gamma \langle \hat{\rho}_\gamma + \hat{\rho}_\gamma^\dagger \rangle (\hat{\rho}_\gamma + \hat{\rho}_\gamma^\dagger), \tag{19}$$

$$\hat{\eta}_- = \sum_{\gamma}^{(2N)^2} \lambda_\gamma \langle \hat{\rho}_\gamma - \hat{\rho}_\gamma^\dagger \rangle (\hat{\rho}_\gamma - \hat{\rho}_\gamma^\dagger), \tag{20}$$

$$\hat{\eta}_0 = \sum_{\gamma}^{(2N)^2} \lambda_\gamma \Big(\langle \hat{\rho}_\gamma + \hat{\rho}_\gamma^\dagger \rangle^2 - \langle \hat{\rho}_\gamma - \hat{\rho}_\gamma^\dagger \rangle^2 \Big). \tag{21}$$

$\hat{\eta}_+$ and $\hat{\eta}_-$ are one body terms, which can be combined with $\hat{H}_1$ in (10). The constant term $\hat{\eta}_0$ can be ignored because it won't affect the physical observables in the sampling process.

After simplification, the total Hamiltonian is therefore

$$\hat{H} = \sum_{\alpha} \hat{H}_{1\alpha} + \hat{H}_2, \tag{22}$$

with

$$\hat{H}_{1\alpha} = \sum_{ij}^{N} T_{i\alpha,j\alpha} \hat{c}_{i\alpha}^\dagger \hat{c}_{j\alpha} - \frac{1}{2}\hat{\rho}_0^\alpha - \mu \sum_i \hat{c}_{i\alpha}^\dagger \hat{c}_{i\alpha} + \frac{1}{2}\sum_{\gamma}^{(2N)^2} \lambda_\gamma \langle \hat{\rho}_\gamma \rangle \hat{\rho}_\gamma^{\dagger\alpha} + \frac{1}{2}\sum_{\gamma}^{(2N)^2} \lambda_\gamma \langle \hat{\rho}_\gamma^\dagger \rangle \hat{\rho}_\gamma^\alpha, \tag{23}$$

and $\hat{H}_2$ is given in (18). The additional superscript α in $\hat{\rho}_\gamma^\alpha$ and $\hat{\rho}_\gamma^{\dagger\alpha}$ means we only pick out the corresponding one-body portion with the correct spin index from the total $\hat{\rho}_\gamma$ and $\hat{\rho}_\gamma^\dagger$ to combine into $\hat{H}_{1\alpha}$. As described above, we can then proceed to decouple $\hat{H}_2$ using a continuous HS transform, and calculate the partition function and observables of interest.

C. Details of Importance Sampling

Starting from (18), after applying the continuous Hubbard-Stratonovich Transformation as in (12), the two body propagator containing the background subtraction term now becomes

$$e^{-\triangle\tau \hat{H}_2} = \prod_{\gamma}^{(2N)^2} \big(\frac{1}{\sqrt{2\pi}}\big)^2 \int_{-\infty}^{\infty}\int_{-\infty}^{\infty} d\phi_{\gamma-} d\phi_{\gamma+} e^{-\frac{\phi_{\gamma+}^2+\phi_{\gamma-}^2}{2}} e^{i\frac{\sqrt{\triangle\tau\lambda_\gamma}}{2}\phi_{\gamma+}[(\hat{\rho}_\gamma+\hat{\rho}_\gamma^\dagger)-\langle\hat{\rho}_\gamma+\hat{\rho}_\gamma^\dagger\rangle]} e^{\frac{\sqrt{\triangle\tau\lambda_\gamma}}{2}\phi_{\gamma-}[(\hat{\rho}_\gamma-\hat{\rho}_\gamma^\dagger)-\langle\hat{\rho}_\gamma-\hat{\rho}_\gamma^\dagger\rangle]}. \tag{24}$$

Introducing a force bias shift to every auxiliary field in the above equation, we obtain

$$\begin{aligned} e^{-\triangle\tau \hat{H}_2} &= \prod_{\gamma}^{(2N)^2} \big(\frac{1}{\sqrt{2\pi}}\big)^2 \int_{-\infty}^{\infty}\int_{-\infty}^{\infty} d\phi_{\gamma-} d\phi_{\gamma+} e^{-\frac{(\phi_{\gamma+}-\bar{\phi}_{\gamma+})^2+(\phi_{\gamma-}-\bar{\phi}_{\gamma-})^2}{2}} e^{i\frac{\sqrt{\triangle\tau\lambda_\gamma}}{2}(\phi_{\gamma+}-\bar{\phi}_{\gamma+})[(\hat{\rho}_\gamma+\hat{\rho}_\gamma^\dagger)-\langle\hat{\rho}_\gamma+\hat{\rho}_\gamma^\dagger\rangle]} \times \\ &\qquad e^{\frac{\sqrt{\triangle\tau\lambda_\gamma}}{2}(\phi_{\gamma-}-\bar{\phi}_{\gamma-})[(\hat{\rho}_\gamma-\hat{\rho}_\gamma^\dagger)-\langle\hat{\rho}_\gamma-\hat{\rho}_\gamma^\dagger\rangle]} \\ &= \prod_{\gamma}^{(2N)^2} \big(\frac{1}{\sqrt{2\pi}}\big)^2 \int_{-\infty}^{\infty}\int_{-\infty}^{\infty} d\phi_{\gamma-} d\phi_{\gamma+} p(\phi_{\gamma+},\phi_{\gamma-}) W'(\phi_{\gamma+},\bar{\phi}_{\gamma+},\phi_{\gamma-},\bar{\phi}_{\gamma-}) \hat{B}(\phi_{\gamma+}-\bar{\phi}_{\gamma+},\phi_{\gamma-}-\bar{\phi}_{\gamma-}), \end{aligned} \tag{25}$$

where

$$W'(\phi_{\gamma+},\bar{\phi}_{\gamma+},\phi_{\gamma-},\bar{\phi}_{\gamma-}) = e^{-\frac{\bar{\phi}_{\gamma+}^2+\bar{\phi}_{\gamma-}^2}{2}} e^{\bar{\phi}_{\gamma+}\phi_{\gamma+}+\bar{\phi}_{\gamma-}\phi_{\gamma-}}, \tag{26}$$

contributes to the overall weight of each walker.

D. Obtaining Mean Field Trial Density Matrices and Energies

Observables from mean field theory (MFT) are evaluated using a finite temperature mean field density matrix, which also serves as the trial density matrix for our quantum Monte Carlo simulations. Here, we provide more details on how mean field density matrices are obtained. We can approximate the two body portion of the *ab initio* Hamiltonian by introducing a mean field density matrix, $\bar{D}^{\alpha}_{ij}$, to obtain

$$\frac{1}{2}\sum_{\alpha\beta}\sum_{ijkl}^{N} V_{ijkl}^{\alpha\beta\alpha\beta}\hat{c}^{\dagger}_{i\alpha}\hat{c}_{k\alpha}\hat{c}^{\dagger}_{j\beta}\hat{c}_{l\beta} = \frac{1}{2}\sum_{\alpha\beta}\sum_{ijkl}^{N} V_{ijkl}^{\alpha\beta\alpha\beta}(\hat{c}^{\dagger}_{i\alpha}\hat{c}_{k\alpha} - \bar{D}^{\alpha}_{ik})(\hat{c}^{\dagger}_{j\beta}\hat{c}_{l\beta} - \bar{D}^{\beta}_{jl}) + \frac{1}{2}\sum_{\alpha}(\hat{\rho}^{\alpha}_{MF1} + \hat{\rho}^{\alpha}_{MF2}) - \frac{1}{2}\hat{\rho}_{MF0}, \quad (27)$$

where $\hat{\rho}^{\alpha}_{MF1}$, $\hat{\rho}^{\alpha}_{MF2}$ and $\hat{\rho}_{MF0}$ are the one body and constant terms,

$$\hat{\rho}^{\alpha}_{MF1} = \sum_{ik}\left(\sum_{jl}^{N}\sum_{\beta} V_{ijkl}^{\alpha\beta\alpha\beta}\bar{D}^{\beta}_{jl}\right)\hat{c}^{\dagger}_{i\alpha}\hat{c}_{k\alpha}, \quad (28)$$

$$\hat{\rho}^{\alpha}_{MF2} = \sum_{ik}\left(\sum_{jl}^{N}\sum_{\beta} V_{jilk}^{\beta\alpha\beta\alpha}\bar{D}^{\beta}_{jl}\right)\hat{c}^{\dagger}_{i\alpha}\hat{c}_{k\alpha}; \quad (29)$$

$$\hat{\rho}_{MF0} = \sum_{\alpha\beta}\sum_{ijkl}^{N} V_{ijkl}^{\alpha\beta\alpha\beta}\bar{D}^{\alpha}_{ik}\bar{D}^{\beta}_{jl}. \quad (30)$$

The one body terms may be combined with the kinetic operator, while the constant term can be added at the end of any total energy calculation.

Invoking the mean field approximation means that we ignore the remaining two body term $\frac{1}{2}\sum_{\alpha\beta}\sum_{ijkl}^{N} V_{ijkl}^{\alpha\beta\alpha\beta}(\hat{c}^{\dagger}_{i\alpha}\hat{c}_{k\alpha} - \bar{D}^{\alpha}_{ik})(\hat{c}^{\dagger}_{j\beta}\hat{c}_{l\beta} - \bar{D}^{\beta}_{jl})$, which is a small contribution representing the deviation of the system from the mean field solution. This yields the final mean field Hamiltonian

$$\hat{H}_{MF} = \sum_{\alpha}\sum_{ij}^{N} T_{i\alpha,j\alpha}\hat{c}^{\dagger}_{i\alpha}\hat{c}_{j\alpha} - \frac{1}{2}\sum_{\alpha}\hat{\rho}^{\alpha}_{0} + \frac{1}{2}\sum_{\alpha}\left(\hat{\rho}^{\alpha}_{MF1} + \hat{\rho}^{\alpha}_{MF2}\right) - \frac{1}{2}\hat{\rho}_{MF0}, \quad (31)$$

which can be solved easily at finite temperature to obtain its related mean field density matrix $\bar{D}^{\alpha}_{ij}$. This density matrix can then be used to construct a new Hamiltonian $\hat{H}_{MF}$ given by (31). To obtain the final mean field density matrix, we therefore must iterate this procedure until we achieve convergence: first, we obtain an estimate of the density matrix, then, we form a new Hamiltonian, then, we obtain a new estimate of the density matrix, and so on. When this process is finished, we arrive at a self-consistent mean field solution for $\bar{D}^{\alpha}_{ij}$, which we can use as a trial density matrix for performing background subtraction, or from which we can directly measure observables. Note that at low temperature, the self-consistent process may be difficult to converge. We use a linear density mixing scheme to improve the convergence.

E. Proof of the Positive Semi-Definiteness of the *Ab Initio* Supermatrix

Elements of an *ab initio* supermatrix $\mathbf{V}$ are defined by

$$V_{(i\alpha,k\alpha),(l\beta,j\beta)} = \int d\vec{r}_1 d\vec{r}_2 \phi^{*}_{i\alpha}(\vec{r}_1)\phi^{*}_{j\beta}(\vec{r}_2)\frac{1}{|\vec{r}_1 - \vec{r}_2|}\phi_{k\alpha}(\vec{r}_1)\phi_{l\beta}(\vec{r}_2), \quad (32)$$

where $\vec{r}_i$ represents the spatial coordinates of the i-th electron, and $\phi_{i\alpha}$ is the $i\alpha$-th spin-orbital basis function.

For any vector $\mathbf{u}$,

$$\begin{aligned}
\mathbf{u}^T\mathbf{V}\mathbf{u} &= \sum_{(i\alpha,k\alpha),(l\beta,j\beta)} u_{(k\alpha,i\alpha)}V_{(i\alpha,k\alpha),(l\beta,j\beta)}u_{(l\beta,j\beta)} \\
&= \int d\vec{r}_1 d\vec{r}_2 \frac{1}{|\vec{r}_1 - \vec{r}_2|}\left(\sum_{(i\alpha,k\alpha)} u_{(k\alpha,i\alpha)}\phi^{*}_{i\alpha}(\vec{r}_1)\phi_{k\alpha}(\vec{r}_1)\right)\left(\sum_{(l\beta,j\beta)} u_{(l\beta,j\beta)}\phi^{*}_{j\beta}(\vec{r}_2)\phi_{l\beta}(\vec{r}_2)\right) \\
&= \int d\vec{r}_1 d\vec{r}_2 \frac{1}{|\vec{r}_1 - \vec{r}_2|} f(\vec{r}_1)f(\vec{r}_2)
\end{aligned} \quad (33)$$

where we have substituted (32) in the second line, and define $f(\vec{r}) \equiv \sum_{(i\alpha,k\alpha)} u_{(k\alpha,i\alpha)} \phi^*_{i\alpha}(\vec{r})\phi_{k\alpha}(\vec{r})$.

The Coulomb interaction $1/|\vec{r}_1 - \vec{r}_2|$ can be further written as an integral over a Gaussian kernel, which gives

$$\frac{1}{|\vec{r}_1 - \vec{r}_2|} = \int_0^\infty dt \frac{1}{\sqrt{2\pi t^3}} e^{-\frac{|\vec{r}_1 - \vec{r}_2|^2}{2t}}. \tag{34}$$

Substituting (34) into (33), and applying the Fubini-Tonelli Theorem to exchange the integration order, we obtain

$$\mathbf{u}^T \mathbf{V} \mathbf{u} = \int_0^\infty dt \frac{1}{\sqrt{2\pi t^3}} \left(\int d\vec{r}_1 d\vec{r}_2 e^{-\frac{|\vec{r}_1 - \vec{r}_2|^2}{2t}} f(\vec{r}_1) f(\vec{r}_2) \right). \tag{35}$$

Note that the function $f(\vec{r})$ defined here is physically well conditioned and is square-integrable, namely $f \in L^2$. From the basic properties of Gaussian kernels, we know that the integral in the parentheses in (35) is non-negative,

$$\int d\vec{r}_1 d\vec{r}_2 e^{-\frac{|\vec{r}_1 - \vec{r}_2|^2}{2t}} f(\vec{r}_1) f(\vec{r}_2) \geq 0, \tag{36}$$

as long as $t > 0$. Substituting (36) into (35), we immediately have

$$\mathbf{u}^T \mathbf{V} \mathbf{u} \geq 0, \tag{37}$$

for any $\mathbf{u}$. This definitively demonstrates that the *ab initio* supermatrix $\mathbf{V}$ is positive semi-definite.

Note that for model systems such as Hubbard model, the Coulomb interaction is usually truncated or screened to a short range (or on-site) effective interaction, so that the transform from the Coulomb interaction to the Gaussian integral cannot readily be performed and thus that the above proof is not directly applicable. We indeed observe the ramifications of this fact in numerical simulations: the supermatrix of the Hubbard model is not positive semi-definite, and both negative and positive eigenvalues can appear.

F. Tabulated Data for Figures in the Main Text

In the following, all of the data used to generate the figures in the main text are provided. It should be noted that all of the following calculations were performed by first finding a chemical potential that corresponds to a given number of electrons and then computing ED, AFQMC, and MFT energies. Depending upon the chemical potentials used, this may introduce slight deviations in the energies provided as compared with theoretically exact energies obtained within the canonical ensemble.

TABLE I. The internal energy (Hartree) of H_2O in the STO-3G basis.

$1/k_BT$	ED	AFQMC	MFT
0.01	-61.657841	-61.66(4)	-61.564377
0.1	-69.709056	-69.69(4)	-69.162930
0.2	-71.907839	-71.90(1)	-71.516931
0.5	-72.662457	-72.66(1)	-72.244073
1	-73.151258	-73.11(2)	-72.566542
2	-73.775883	-73.76(2)	-73.105678
5	-74.544744	-74.55(2)	-74.023591
10	-74.947094	-74.92(2)	-74.568453
16	-75.019015	-74.98(3)	-74.789765
20	-75.023360	-75.02(3)	-74.856005
25	-75.024138	-75.02(4)	-74.900785
33.3	-75.024235	-75.02(5)	-74.932375

TABLE II. The internal energy (Hartree) of C_2 in the STO-6G basis. The exact non-relativistic, ground state energy is -75.434537 Hartree.

$1/k_BT$	AFQMC	MFT
0.01	-72.0633(8)	-72.043783
0.1	-72.271(6)	-72.103403
1	-73.46(3)	-72.700859
2	-74.11(4)	-73.274621
5	-74.91(7)	-74.170179
10	-75.22(3)	-74.646035
16	-75.36(5)	-74.839024
20	-75.32(6)	-74.882408
25	-75.4(1)	-74.907618
33.3	-75.6(2)	-74.929173

TABLE III: Occupancy, N, of the nitrogen atom vs. chemical potential, μ, in the STO-6G basis at different temperatures. All temperatures and chemical potentials are in Hartree.

μ	N at $k_BT = 1.0$	Error Bar	N at $k_BT = 0.1$	Error Bar
-5.0	+2.775517	+0.015649	+2.00000	+0.000000
-4.9	+2.827576	+0.017226	+2.000001	+0.000000
-4.8	+2.883171	+0.009734	+2.000004	+0.000001
-4.7	+2.934897	+0.016942	+2.000007	+0.000004
-4.6	+2.994263	+0.016652	+2.000016	+0.000009
-4.5	+3.056489	+0.018124	+2.000024	+0.000021
-4.4	+3.120466	+0.016452	+2.000123	+0.000061
-4.3	+3.181369	+0.021359	+2.000364	+0.000143
-4.2	+3.249204	+0.018402	+2.001005	+0.000281
-4.1	+3.310359	+0.023132	+2.002860	+0.000471
-4.0	+3.383610	+0.011025	+2.006538	+0.000821
-3.9	+3.447899	+0.022447	+2.017944	+0.001406
-3.8	+3.515682	+0.018598	+2.045490	+0.002697
-3.7	+3.587622	+0.012760	+2.116417	+0.005189
-3.6	+3.670765	+0.019860	+2.293460	+0.012844
-3.5	+3.742075	+0.024122	+2.508752	+0.020233
-3.4	+3.822000	+0.018956	+2.747936	+0.036301
-3.3	+3.893970	+0.017796	+2.871995	+0.035952
-3.2	+3.981393	+0.024583	+2.962444	+0.035956
-3.1	+4.050298	+0.017449	+3.035517	+0.029312
-3.0	+4.133964	+0.026042	+3.082995	+0.030354
-2.9	+4.212235	+0.025142	+3.189069	+0.036420
-2.8	+4.294585	+0.029541	+3.392010	+0.043118
-2.7	+4.375589	+0.017649	+3.655683	+0.043982
-2.6	+4.456201	+0.026611	+3.879189	+0.033892
-2.5	+4.545911	+0.022001	+3.927999	+0.023130
-2.4	+4.623642	+0.021501	+3.970532	+0.018830
-2.3	+4.713916	+0.029229	+4.009007	+0.016552
-2.2	+4.798170	+0.028920	+4.037212	+0.015280
-2.1	+4.880419	+0.029298	+4.115878	+0.018671
-2.0	+4.968512	+0.024441	+4.267119	+0.022468
-1.9	+5.052326	+0.022334	+4.544293	+0.031251
-1.8	+5.139253	+0.030539	+4.762987	+0.033040
-1.7	+5.227688	+0.051572	+4.866220	+0.028355
-1.6	+5.314192	+0.018927	+4.955101	+0.028558
-1.5	+5.403660	+0.021306	+5.030537	+0.030934
-1.4	+5.489782	+0.025974	+5.098210	+0.035223
-1.3	+5.578366	+0.028326	+5.190183	+0.047100
-1.2	+5.666919	+0.032740	+5.420303	+0.053071
-1.1	+5.754146	+0.020159	+5.665965	+0.048751
-1.0	+5.843856	+0.011771	+5.882139	+0.046855
-0.9	+5.931309	+0.026743	+5.934199	+0.044811
-0.8	+6.019431	+0.034100	+6.034486	+0.043969
-0.7	+6.107615	+0.028906	+6.106881	+0.062831
-0.6	+6.195266	+0.017643	+6.149598	+0.072681

-0.5	+6.281296	+0.028198	+6.406233	+0.093832
-0.4	+6.372849	+0.029871	+6.583948	+0.103595
-0.3	+6.459179	+0.038297	+6.786758	+0.068000
-0.2	+6.547036	+0.032811	+6.918219	+0.077881
-0.1	+6.633839	+0.018306	+6.965226	+0.034042
+0.0	+6.722513	+0.026833	+7.008555	+0.034042
+0.1	+6.806090	+0.029384	+7.116937	+0.056651
+0.2	+6.898661	+0.027031	+7.368022	+0.145205
+0.3	+6.982928	+0.034052	+7.461403	+0.143748
+0.4	+7.063049	+0.040539	+7.843200	+0.124731
+0.5	+7.153682	+0.027810	+7.985141	+0.107265
+0.6	+7.238487	+0.037560	+8.038756	+0.078324
+0.7	+7.327173	+0.029914	+8.016139	+0.028747
+0.8	+7.412065	+0.022930	+8.063458	+0.025271
+0.9	+7.489670	+0.021011	+8.120954	+0.096210
+1.0	+7.570864	+0.020641	+8.255501	+0.192727
+1.1	+7.658912	+0.011750	+8.709194	+0.135730
+1.2	+7.736232	+0.027300	+8.817749	+0.091703
+1.3	+7.822420	+0.018079	+8.994548	+0.048407
+1.4	+7.898839	+0.014423	+9.026712	+0.046844
+1.5	+7.974030	+0.034715	+9.041305	+0.041363
+1.6	+8.056038	+0.014513	+9.090873	+0.039118
+1.7	+8.135464	+0.032067	+9.208324	+0.035563
+1.8	+8.208452	+0.021635	+9.482027	+0.021857
+1.9	+8.286496	+0.017512	+9.674730	+0.012889
+2.0	+8.356670	+0.010235	+9.860978	+0.005590
+2.1	+8.426331	+0.031939	+9.946095	+0.002697
+2.2	+8.501034	+0.015649	+9.977586	+0.001392
+2.3	+8.574974	+0.016645	+9.991786	+0.001019
+2.4	+8.640520	+0.015122	+9.997221	+0.000455
+2.5	+8.706805	+0.016108	+9.998957	+0.000274
+2.6	+8.771075	+0.015997	+9.999569	+0.000133
+2.7	+8.840801	+0.023600	+9.999879	+0.000060
+2.8	+8.900054	+0.015195	+9.999953	+0.000022
+2.9	+8.963548	+0.021800	+9.999999	+0.000008
+3.0	+9.018084	+0.011670	+9.999992	+0.000003
+3.1	+9.081703	+0.012430	+9.999999	+0.000001
+3.2	+9.135721	+0.015993	+9.999999	+0.000001
+3.3	+9.187430	+0.016366	+9.999999	+0.000000
+3.4	+9.240778	+0.013390	+10.00000	+0.00000
+3.5	+9.287409	+0.011733	+10.00000	+0.00000
+3.6	+9.337543	+0.016078	+10.00000	+0.00000
+3.7	+9.380295	+0.008802	+10.00000	+0.00000
+3.8	+9.422328	+0.007795	+10.00000	+0.00000
+3.9	+9.462889	+0.009757	+10.00000	+0.00000
+4.0	+9.499485	+0.010482	+10.00000	+0.00000

TABLE IV. The internal energy (Hartree) of H_{10} in the STO-6G basis at its equilibrium bond length of 1.786 a.u. The exact, non-relativistic ground state energy is -5.424570 Hartree.

$1/k_BT$	AFQMC	MFT
0.01	0.0803(9)	0.093683
0.1	-0.151(4)	-0.027001
1	-2.01(1)	-1.219754
2	-3.29(2)	-2.353559
5	-4.77(3)	-4.105092
10	-5.30(5)	-4.841360
16	-5.38(4)	-5.059083
20	-5.38(2)	-5.117851
25	-5.44(6)	-5.161809
33.3	-5.41(2)	-5.204183

TABLE V. The internal energy (Hartree) of H_{10} in the STO-6G basis at a stretched bond length of 2.4 a.u. The exact non-relativistic, ground state energy is -5.227936 Hartree.

$1/k_BT$	AFQMC	MFT
0.01	-1.7488(2)	-1.739656
0.1	-1.865(1)	-1.773753
0.2	-1.981(3)	-1.811868
0.5	-2.287(4)	-1.927442
1	-2.723(9)	-2.122643
2	-3.41(3)	-2.510962
5	-4.38(3)	-3.483536
10	-4.91(4)	-4.289207
16	-5.14(4)	-4.620001
20	-5.13(3)	-4.714858
25	-5.19(5)	-4.780650
33.3	-5.2(1)	-4.837063

TABLE VI. The internal energy of a 4×2 single-band Hubbard model with $U/t = 4$ at half filling on a square lattice. All energies are in units of t.

$1/k_BT$	AFQMC	MFT
0.01	7.80(2)	7.880007
0.1	6.03(3)	6.806939
1	-2.8(2)	-0.203592
2	-4.3(1)	-2.539894
4	-5.7(1)	-3.784092
10	-5.9(1)	-3.999455
20	-5.9(1)	-4.000000
25	-6.0(1)	-4.000000

TABLE VII. The internal energy of a 4×2 two-band Hubbard-Kanamori model with $U/t = 4, J/t = 1$ at half filling on a square lattice. All energies are in units of t.

$1/k_BT$	AFQMC	MFT
0.01	27.53(6)	27.760014
0.1	23.5(1)	25.613879
1	5.2(3)	11.592815
2	1.1(5)	6.920213
4	-1.1(3)	4.431817
10	-0.8 (6)	4.001090
16	-0.6 (5)	4.000003

TABLE VIII. Average absolute value of the phase angle (Degrees) for various *ab initio* systems at different temperatures, under free propagation and background subtraction. Slashes indicate that error bars were not able to be converged for the given system.

	Free Propagation		Background Subtraction			
$1/k_BT$	H_2O	C_2	H_2O	C_2	H_{10} (Equilibrium)	H_{10} (Stretched)
0.01	41.8(9)	26.3(6)	0.030(2)	4.3(5)E-6	5.3(1)E-4	3.9(1)E-6
1	91(2)	89(2)	3.4(7)	0.6(3)	1.03(4)	0.40(1)
2	89(2)	89(2)	8(1)	2.2(8)	3.6(1)	1.58(5)
5	/	/	27(1)	11(1)	14.4(6)	10.9(3)
10	/	/	46(1)	29(2)	28.4(7)	29.5(6)
16	/	/	53(1)	56(2)	37.7(7)	41.6(7)
20	/	/	57(1)	74(2)	40.2(7)	57.1(9)
25	/	/	58(1)	73(2)	54.2(8)	50.6(8)
33.3	/	/	64(1)	75(1)	53.2(9)	74(1)

G. Tabulated Data for Other First and Second Row Atoms and Molecules

Benchmark results for other first and second row atoms in the periodic table not discussed in the text and H_2 are provided below at various inverse temperatures, computed using ED, AFQMC, and MFT.

TABLE IX. The internal energy (Hartree) of H_2 in the STO-3G Basis.

$1/k_BT$	ED	AFQMC	MFT
0.01	-0.608951	-0.6090(1)	-0.608298
0.1	-0.616675	-0.6168(4)	-0.610226
1	-0.686456	-0.6862(6)	-0.629880
5	-0.870669	-0.871(2)	-0.720445
10	-0.974220	-0.972(3)	-0.823580
20	-1.048646	-1.047(4)	-0.957009
50	-1.066490	-1.069(2)	-1.038881
100	-1.066602	-1.072(7)	-1.041605

TABLE X. The internal energy (Hartree) of the helium atom in the MIDI Basis.

$1/k_BT$	ED	AFQMC	MFT
0.01	-0.212171	-0.2118(7)	-0.207955
0.1	-0.370275	-0.366(3)	-0.327364
0.2	-0.545960	-0.543(2)	-0.460965
0.5	-1.047245	-1.036(6)	-0.858395
1	-1.722136	-1.715(5)	-1.462187
2	-2.502106	-2.506(5)	-2.276931
5	-2.846430	-2.846(3)	-2.813331
10	-2.850574	-2.851(4)	-2.835515
20	-2.850577	-2.851(5)	-2.835598
50	-2.850577	-2.853(5)	-2.835598

TABLE XI. The internal energy (Hartree) of the lithium atom in the MIDI Basis.

β	ED	AFQMC	MFT
0.01	-4.527322	-4.527(2)	-4.524944
0.05	-4.650689	-4.650(3)	-4.637345
0.1	-4.800995	-4.801(5)	-4.771334
0.2	-5.085673	-5.084(8)	-5.018451
0.5	-5.787149	-5.79(1)	-5.615290
1	-6.535186	-6.528(7)	-6.270235
2	-7.152696	-7.148(5)	-6.920131
5	-7.288515	-7.2808(6)	-7.253609
10	-7.335787	-7.3218(6)	-7.289847
20	-7.387277	-7.367(1)	-7.328862
50	-7.415739	-7.385(3)	-7.365749
100	-7.418664	-7.384(2)	-7.393584

TABLE XII. The internal energy (Hartree) of the boron atom in the MIDI Basis.

β	ED	AFQMC	MFT
0.01	-11.082440	-11.08(1)	-11.080260
0.1	-13.917083	-13.93(4)	-13.752883
0.2	-16.875802	-16.88(5)	-16.377219
0.5	-21.866141	-21.85(3)	-21.033821
1	-23.240278	-23.236(9)	-22.891464
2	-23.591185	-23.57(1)	-23.236813
5	-24.100273	-24.08(2)	-23.722880
10	-24.336156	-24.32(3)	-24.021959
20	-24.426170	-24.4(1)	-24.198037
50	-24.455867	-24.6(3)	-24.250785
100	-24.462663	-24.3(2)	-24.273218

TABLE XIII. The internal energy (Hartree) of the carbon atom in the MIDI Basis. The slash indicates that numerical underflow or overflow occurs at the corresponding temperature.

β	ED	AFQMC	MFT
0.01	-19.206839	-19.22(2)	-19.191994
0.1	-25.185109	-25.17(6)	-24.725267
0.2	-30.220594	-30.19(6)	-29.280635
0.5	-35.001762	-34.91(1)	-34.271457
1	-35.742693	-35.75(1)	-35.225802
2	-36.444645	-36.43(2)	-35.843619
5	-37.231883	-37.23(3)	-36.731085
10	-37.435310	-37.50(6)	-37.011903
20	-37.498072	-37.6(4)	-37.078776
50	-37.512651	-37.4(3)	-37.081044
100	-37.514843	/	-37.081044

TABLE XIV. The internal energy (Hartree) of the nitrogen atom in the MIDI Basis. The slash indicates that numerical underflow or overflow occurs at the corresponding temperature.

β	ED	AFQMC	MFT
0.01	-30.592444	-30.60(2)	-30.552265
0.1	-41.066521	-41.05(7)	-40.218672
0.2	-47.408502	-47.39(4)	-46.282256
0.5	-50.717899	-50.70(2)	-50.074317
1	-51.729096	-51.69(2)	-50.946742
2	-52.956080	-52.94(2)	-52.183746
5	-53.891886	-54.00(3)	-53.340733
10	-54.047597	-54.0(1)	-53.499021
20	-54.109484	-53.6(6)	-53.515755
33.3	-54.136716	-54.2(4)	-53.519663
50	-54.153396	-53.9(5)	-53.526544
100	-54.167023	/	-53.559940

TABLE XV. The internal energy (Hartree) of the oxygen atom in the MIDI Basis. The slash indicates that numerical underflow or overflow occurs at the corresponding temperature.

β	ED	AFQMC	MFT
0.01	-46.029567	-46.03(6)	-45.948682
0.1	-61.673823	-61.67(7)	-60.517364
0.2	-67.666379	-67.66(3)	-66.682083
0.5	-69.976063	-69.95(2)	-69.122111
1	-71.532594	-71.50(3)	-70.513328
2	-73.308290	-73.32(3)	-72.441522
5	-74.307581	-74.35(4)	-73.756461
10	-74.406445	-74.3(1)	-73.824955
20	-74.435497	-74.4(3)	-73.827113
33.3	-74.441517	-73.7(6)	-73.827118
50	-74.443573	/	-73.827118
100	-74.444625	/	/

TABLE XVI. The internal energy (Hartree) of the fluorine atom in the MIDI Basis. The slash indicates that numerical underflow or overflow occurs at the corresponding temperature.

β	ED	AFQMC	MFT
0.01	-65.761204	-65.76(5)	-65.618951
0.1	-86.145314	-86.12(7)	-84.901888
0.2	-90.802146	-90.78(2)	-89.992038
0.5	-93.122699	-93.09(3)	-92.028526
1	-95.473340	-95.44(4)	-94.288254
2	-97.893048	-97.90(3)	-97.038210
5	-98.862027	-98.83(3)	-98.446321
10	-98.922403	-98.9(1)	-98.473558
20	-98.936059	-98.8(2)	-98.474385
25	-98.936614	-99.1(4)	-98.474813
33.3	-98.936928	/	-98.475728
50	-98.937363	/	-98.478298
100	-98.938512	/	-98.490596

TABLE XVII. The internal energy (Hartree) of the neon atom in the MIDI Basis. The slash indicates that numerical underflow or overflow occurs at the corresponding temperature.

β	ED	AFQMC	MFT
0.01	-115.219180	-115.218(3)	-115.154574
0.1	-116.435430	-116.43(1)	-115.913272
0.2	-117.606155	-117.60(2)	-116.752691
0.5	-120.446996	-120.43(3)	-119.149895
1	-123.662816	-123.62(4)	-122.371375
2	-126.701453	-126.69(3)	-125.813576
5	-127.889630	-127.88(2)	-127.649640
10	-127.905179	-127.88(4)	-127.757574
20	-127.905199	-127.92(5)	-127.758803
50	-127.905199	-127.9(1)	-127.758803
100	-127.905199	/	-127.758803

H. Computational Scaling

As mentioned in the main text, our method scales as O(N^3)–O(N^4), where N is the number of orbitals (basis set size). As with most quantum Monte Carlo algorithms, this scaling stems from the fact that our algorithm requires a large number of matrix multiplications, inversions (using LU factorization), and diagonalizations, all of which have an O(N^3) scaling. The CPU time vs. the number of orbitals for several systems is summarized and plotted with a log scale in Figure 1 below, illustrating a typical quantum Monte Carlo power law scaling.

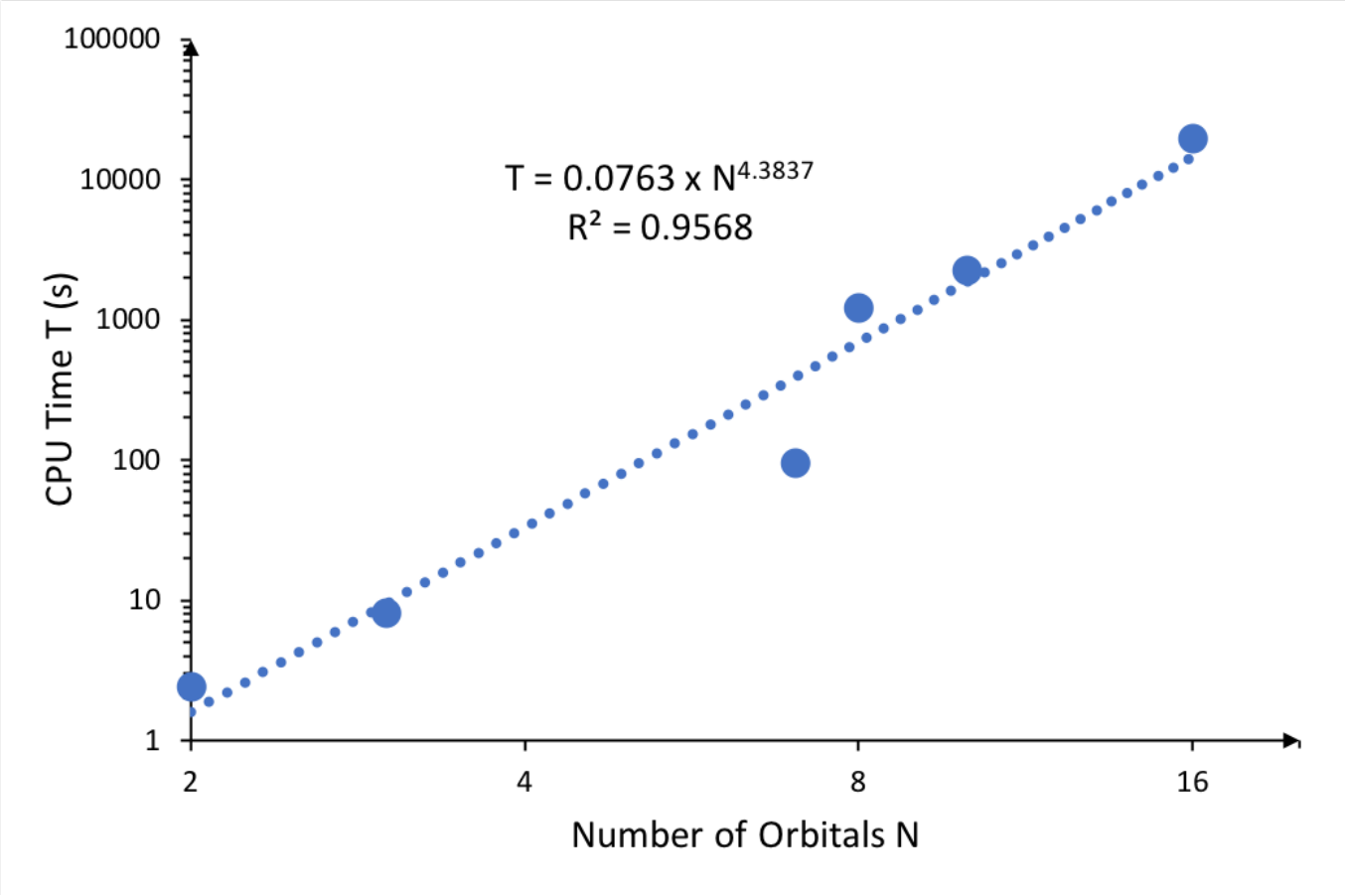

FIG. 1. CPU time vs. number of orbitals for H_2 (STO-3G, N=2), Be (MIDI, N=3), H_2O (STO-3G, N=7), C_2(STO-6G, N=8), H_{10} (STO-6G, N=10), and the 4x2 2-orbital Hubbard-Kanamori model (N=16) at $\beta = 1$, $\Delta\tau = 0.05$ with 128 walkers and 10 blocks, where N is the total number of orbitals in the basis. Dashed line is a fitting that illustrates power law scaling. Note that the y-axis is given using a log scale.

I. Calculation of Statistical Errors

In our finite temperature AFQMC, each walker samples the auxiliary field space and carries information about physical observables. We call propagation in imaginary time from inverse temperature 0 to β one *block*. The calculation is repeated M times to get M blocks, and N *walkers* are used per block. To calculate the error bar on physical observables (internal energy in our case), we first average the internal energy over all N walkers within each block as E_i, where $i = 1, 2, ..., M$. Then, from standard error analysis, the error bar on the average internal energy is obtained as

$$\sigma = \sqrt{\frac{\sum_{i=1}^{M}(E_i - \bar{E})^2}{(M-1)M}}, \tag{38}$$

where $\bar{E}$ is the mean of the internal energy. Note that, while more sophisticated error analyses that address correlations among samples, such as reblocking, exist, we believe that our simple model of statistical independence will still provide sound observable estimates.